

A Method to Characterise Jets Using Correlations of Large-Scale Features in Instantaneous Planar Images

C.H. Birzer, P.A.M. Kalt and G.J. Nathan

The School of Mechanical Engineering
The University of Adelaide, South Australia, 5005, Australia

Abstract

An approach to characterise jets by analysis of the locations of large-scale features identified in images of the instantaneous flow field is presented. A frequency domain is generated from the correlations of identified large-scale features in ensembles of instantaneous planar images. The frequency-domain correlation image provides a measure of the underlying large-scale features; namely the characteristic distances and angles between large-scale features, number densities of large-scale features in the image field, variations in distance between large-scale features and their dominant mode. The approach is assessed analytically and applied to experimental data. Results show that the proposed method can be used successfully to characterise the large-scale features of jet flows.

Introduction

Mixing of fuel and air is commonly achieved using turbulent jets. These mixing processes are complex, comprising both large- and small-scale turbulent features that control the instantaneous distribution of fuel and air. These features have a controlling influence on many aspects of combustion, such as heat release and pollutant formation. It is therefore necessary to classify the structure of instantaneous jet flows. Jets are generally classified by the characteristic parameters of half-width rates of centreline decay and the higher order statistics along the axis. However, these parameters are derived from single point measurements and provide little information of the instantaneous flow structure. The advent of a range of planar measurement techniques opens the door to a range of methods, but there remains a need for other processing methods to better resolve underlying structure. The aim of the current paper is to present a technique to characterise jets based on the correlations of instantaneous large-scale features identified in planar images.

Compared with homogeneously distributed flows, the formation of rich and / or lean fuel regions can significantly influence thermal and chemical properties, such as ignition temperatures, heat transfer and emissions productions [1,5,9,10]. Control of the structure of instantaneous fuel distribution offers a means to reduce the production of harmful pollutant emissions and improve heat transfer. Therefore, statistical analysis of the formation of structures from different nozzle designs may enable further optimisation of combustion systems.

Information about the coherence of structures requires an ensemble of data. For the current work, planar instantaneous images are considered. (By using planar images it is noted that only planar slices of structures are identified. These are termed large-scale features.) The specific information desired relates to the spatial distribution of the large-scale features in a time- or ensemble-resolved sense. This information enables greater understand of flows in order to address questions such as, is there

some general pattern in the vortices shed within a turbulent jet or some pattern in the formation of particle clusters?

In the current paper a method to characterise the coherence of large-scale features found in an ensemble of planar scalar images is proposed. Such images may be of large-scale features identified from fluid concentration, (eg from Planar Laser Induced Fluorescence, PLIF), particle concentrations (eg from planar nephelometry), or vortices (eg from Particle Image Velocimetry, PIV). The requirement is that large-scale features must be resolved from instantaneous planar imaging. Identification of large-scale features from concentrations can be conducted by methods including simple thresholding [11,12] to more advanced methods based on a variance from the mean [3,4].

The current paper presents a method based on the correlation of the large-scale features in images from an ensemble. Auto-correlation and cross-correlation [2,8] use the Fourier transformation to turn a spatial coordinate system (the 2D image) into a 2D frequency space, and the separation of peaks in the frequency space is related to the most common spatial separation over the entire ensemble. For example, PIV [2] uses the Fourier transform to turn an image of particle distributions into a correlation space corresponding to particle displacements, and the displacement can be used to infer velocity of the particles when the time delay is known. However, to the authors' knowledge, no previous method has been reported that applies auto-correlations on large-scale flow features identified from instantaneous images. The aim of the present paper is to present such a method and to assess its effectiveness, using a series of theoretical flow features and then using real experimental data with a view to characterising the underlying structure of a jet.

Methodology

The proposed method uses instantaneous planar images that are processed to identifying flow features. These images are converted to a binary *feature image*, in which values are either unity within an identified large-scale features, or zero elsewhere. A correlation space is then derived from an ensemble of (binary) feature images. The total number of images in the ensemble is M and j denotes the j^{th} image in the ensemble. In each image, $1 \leq j \leq M$, there are n_j identified structures.

If the spatial dimension of each image is $W \times H$, then a frequency domain image is created four-times this size, i.e. $2W \times 2H$. The notation x and y correspond to the coordinates of the spatial domain of the feature image and x' and y' correspond to the coordinates of the frequency domain of the correlation image. The centre of the frequency domain ($x'=W, y'=H$) corresponds to zero displacement.

The auto-correlation of the spatial ensemble is generated by populating the frequency domain with copies of the feature

images. For each large-scale feature in each image, the entire binary feature image is copied into the frequency domain with the centroid of the large-scale feature located at the zero-displacement origin in the correlation space. The centre of the frequency domain is then the self-correlation peak. This process is repeated for the entire ensemble with the one correlation space. The pixel count, S , is equal to the number of overlapping structures. Mathematically this can be represented by the following equation

$$S_{x^T y^T} = \sum_{j=1}^M \sum_{i=1}^{n_j} S_{x^T y^T} \quad (1)$$

where x^T and y^T are the transposed coordinates of the large-scale feature's centre to the centre of the correlation space image. Therefore, the strength of the self-correlation peak will equal the total number of large-scale features in the entire ensemble, n_{TOT} .

$$n_{TOT} = \sum_{j=1}^M n_j \quad (2)$$

Scattered around the self-correlation peak will be a number of secondary peaks corresponding to other typical displacements. In a randomly distributed ensemble, without any coherence, there will be no distinct secondary peaks. In an idealised flow, where the spacing and shapes of the large-scale features are constant, the strength (magnitude) of the secondary peaks will approach the strength of the auto-correlation peak. In addition, if the structure shapes are symmetric about two axes, the frequency space will be rotationally symmetrical around the origin of the frequency domain. This is because any correlation from the centre of structure A to B will have an opposite correlation of equal strength from B to A .

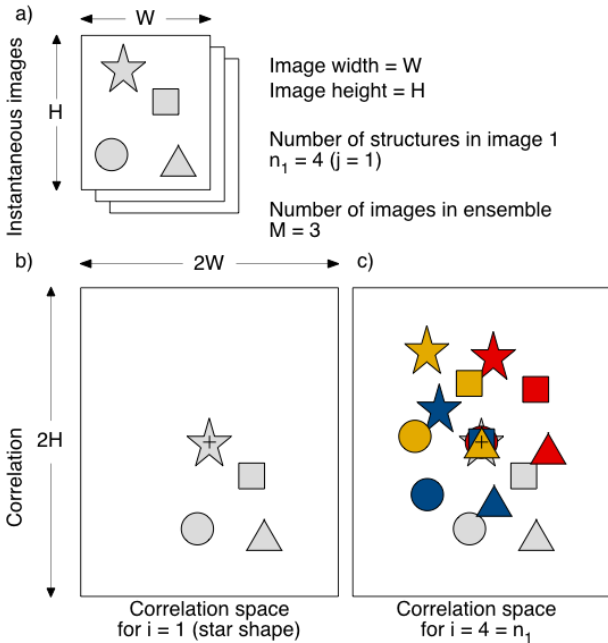


Figure 1. Schematic diagram of the correlation process for a sample image with four features (star, square, circle and triangle). Part a) shows the instantaneous image from an ensemble, part b) the correlation step for the first feature, part c) the correlation of the first image. The colour used in part c) highlights the steps.

Figure 1 illustrates the process schematically. In this example there are only three images in the ensemble ($M = 3$) and only the first image ($j = 1$) is considered. In the first image there are four

features ($n_j = n_1 = 4$): the first feature ($i = 1$) is taken as the star shape.

The centre of the first feature (star) is located at the centre of the correlation space. The remaining structures are located on the correlation space relative to the star as they are in the instantaneous image (figure 1b). This process is repeated for all features in the image and then all images in the ensemble. For the example shown, only the first image is used. Colours are used to differentiate the correlations for each image, and not image pixel count.

In this example, it can be seen that there isn't perfect rotational symmetry due to the various shapes of the features. However, on analysis it can be seen that there is rotational symmetry relative to the features' centroids.

Analytical Results

To evaluate the proposed method, four different idealised examples of flow modes are considered. These modes are termed Axial, Ring, Helical and Random, based on the distribution of the 2-D slices through the features. Instantaneous images of the idealised features are shown in figure 2. These are idealised to provide a constant separation distance between features with the exception of the Random case which has random separations. The corresponding correlations for each case are also shown in figure 2. In these examples the flow is directed vertically. Only one instantaneous image from the ensembles is shown.

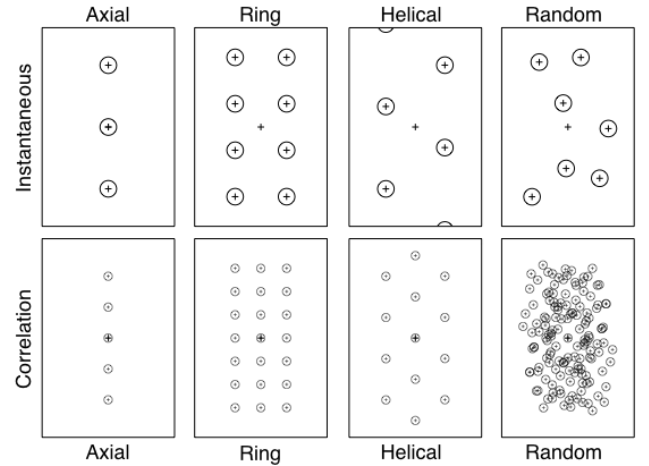


Figure 2. Instantaneous images and correlations of idealised examples of round features with constant separation distance.

From the spacing between the correlation peaks it can be seen that the Axial mode has higher order peaks above and below the correlation space image centre. Not surprisingly, the pattern of the correlation peaks is linear in the vertical direction, which corresponds to the direction of flow. Characteristic separation distances can be determined from the distance between the centre of the correlation peaks and the primary peak. As this example has constant separation distance between features, the separation distance between the correlation peaks is constant.

The correlation of the Ring mode exhibits a clear matrix of rows and columns with characteristic vertical and horizontal separation distances. Based on flow direction, horizontal spacing relates to the horizontal separation distance between pairs of features, while the vertical spacing relates to the frequency of features formation.

The Helical mode results in a uniform pattern of a truncated matrix aligned at 45° . Unlike the Ring mode, there is no secondary peak in the same horizontal plane as the image centre. This is a key difference between Helical and Ring flows. The

distance from the centre of the correlation space to the closest four peaks is the same, as are their angles in each quadrant.

As expected, the correlation pattern for the Random mode is random. There is no characteristic spacing; however, information regarding the minimum separation distance between features can be inferred from the area free of correlation “peaks” around the centre of the correlation space.

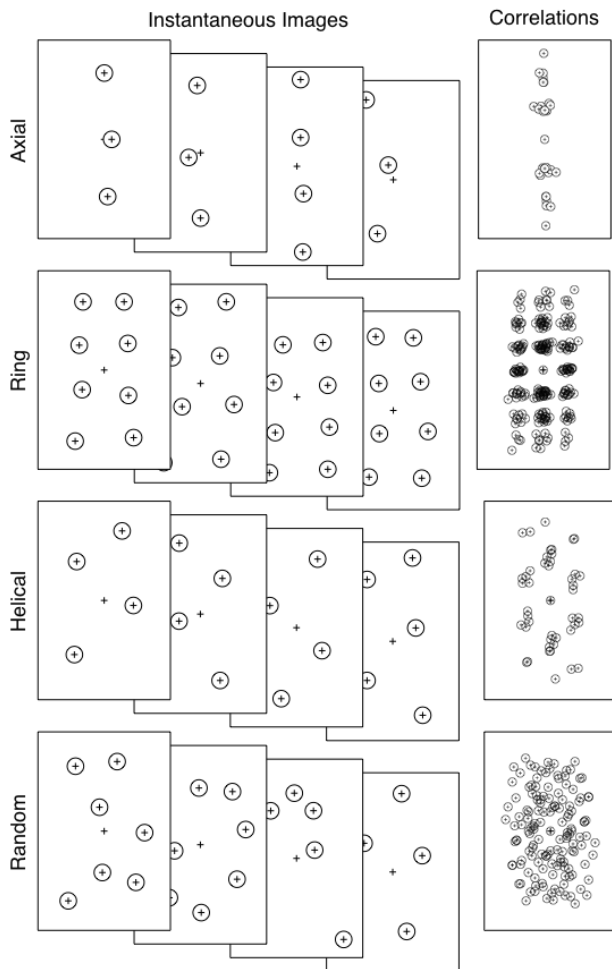


Figure 3. Instantaneous images and correlations of idealised examples of round structure with variations in separation distance.

It is unlikely that real jet flows will have constant separation distance between successive instantaneous large-scale features. Hence the effect of circular shapes without exact separation is assessed. Figure 3 shows four instantaneous images and corresponding correlation images for the four types of modes.

Strong similarities can be seen in the correlations from figures 2 and 3 for each of the Simple, Ring and Helical modes. The rotational symmetry of the frequency domain is still evident and the characteristics separation distances and angles can still be determined. There is obviously no difference in the Random modes of figures 2 and 3.

Next we assess the influence of non-circular and dissimilar shape as well as variation in spacing. Figure 4 shows examples of the same four flow modes, but with variations to the shapes of the features. The same separation distances presented in the examples of figure 3 are used and the ensemble size is still four images, although only one instantaneous image for each flow case is presented. Again, strong similarities in the correlation images of figures 2 and 4 are apparent. Correlation peaks can again be identified and separation distances and angles between

peaks can be calculated. However, the peaks are not as clear or distinct as in figure 2 or figure 3. This may result in less confidence in results, although the peaks can be expected to become clearer with a larger ensemble. It is also noted that the correlation peaks are no longer rotationally symmetric about the image centre, although there is still symmetry of the feature centroids.

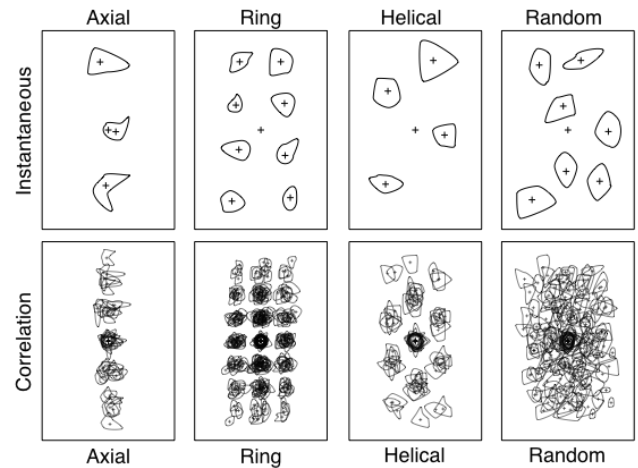


Figure 4. Instantaneous images and correlations of non-circular and dissimilar shapes also with variations in separation distances.

It can be seen from figure 4 that an increase in variability results in a broader central correlation peak that may obscure the weaker side peaks. To avoid this potential problem, the self-correlation peak at the centre of image is excluded from the analysis and only the location of the centroid is marked. This is shown schematically in figure 5. Horizontal and vertical separation distances are labelled L_H and L_V respectively. It is clear that the schematic analysis can be applied to the correlation images in figures 2, 3 and 4.

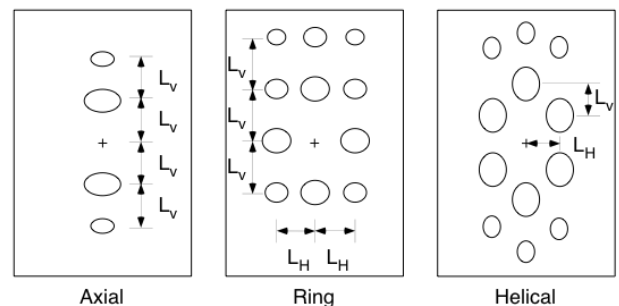


Figure 5. Schematic analysis of the correlation spaces from Simple, Paired, and Helical flows.

Experimental Results

Experimental data have been used to assess the application of the proposed method. These data are images of the particle distributions in the first 13 nozzle diameters of particle-laden jets from two different nozzles: one with swirl air injection and the other with radial air injection. Other than the angle of injection (45° for the swirl flow and 0° for the radial flow) all other initial conditions for the two flows are identical. The particle distributions were imaged using planar nephelometry with corrections for attenuation [6,7]. A smoothing length scale of half the nozzle diameter has been used to identify structures of particle clusters in each image [3,4]. The ensemble size is 131 images for the swirl flow and 186 images for the radial flow.

Figure 5 shows the correlation contours for the clusters identified from the jets with swirl and radial injection. The self-correlation peak has been removed for ease of analysis. Contour lines have

been applied at increments of 20% of the maximum pixel count (excluding the self-correlation peak), with an additional contour line at 90% maximum peak count.

Clear features are evident. For the case of swirl injection, two secondary peaks are detected, at $x'/D \approx \pm 2.1$, i.e. above and below the image centre. Two other peaks are found below the nozzle at $x'/D \approx -1.8$ approximately $\pm 35^\circ$ from the image centre, as well as at $x'/D \approx 1.8$ and approximately 35° from the centreline (i.e. above and to the left of the image centre). Furthermore, there are distinct regions to either side of the image centre with lower pixel intensity. This indicates that the clusters are not paired as expected in Ring mode, but rather distributed in a helical fashion. As the secondary peaks below the image centre are more distinct than those above, the helical nature of the distribution of clusters must be stronger further downstream. These results indicate that the swirl flow has a helical mode with a characteristic separation distance between clusters of approximately two diameters and an angle of $\pm 35^\circ$ in this region of the flow. The pixel count of the central pixel is 1727, therefore there are 1727 clusters in 131 images; an average, 13.2 clusters per image.

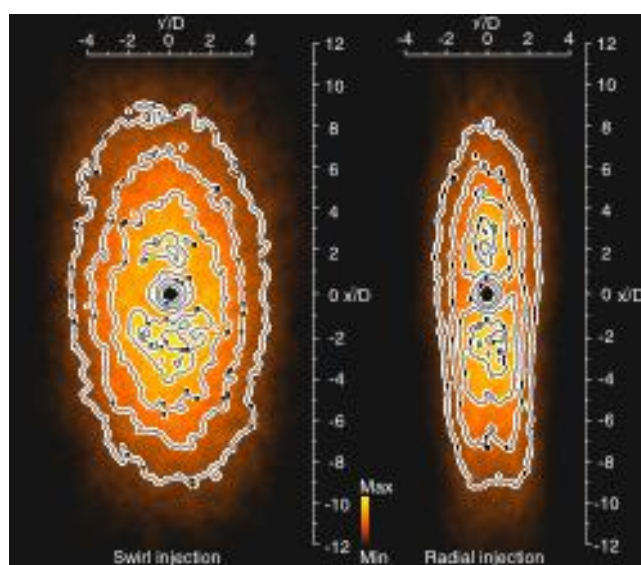


Figure 5. Correlation space from jet flow with swirl injection (left) and radial injection (right).

The flow with radial injection has a narrower distribution than for swirl. The secondary peaks are approximately three nozzle-diameters above and below the image centre. Again, it can be seen that the regions on to the left and right of the image centre have a much lower correlation than those above and below. These results indicate that the radial flow has an Axial mode with characteristics separation distance of $x'/D \approx 3$. The pixel count of the central pixel is 1564, thus for an ensemble of 186 images, there is an average of 8.4 clusters per image.

The results for flows with swirl and radial injection are consistent with expectations. Swirling flows, as expected, shows a Helical mode, while radial injection to a simple jet produces an Axial mode. Importantly, the separation distance between clusters is smaller for flows with swirl injection than for those with radial injection. Furthermore, swirl injection results in the formation of 60% more clusters than for radial injection.

Conclusions

A method has been developed to characterise jets based on the correlations of instantaneous large-scale features identified from planar images. It uses a correlation about the centroid of each identified large-scale feature with the remaining features in each instantaneous image. Four generic flow cases are assessed to

provide analytical solutions. Data from two experimental cases are also assessed. The results show that the analytical solutions are applicable to experimental results. The results provide an indication of the characteristic separation distances and angles between features, the number density of features and the typical distribution of features in the flow. These characteristics are important to understanding and optimising combustion, as well as other fundamental and applied studies.

An advantage of the proposed method is that it can be used to identify patterns that are not clearly evident from simple visual inspection of instantaneous images. This is because the underlying features exhibit considerable instantaneous variability. Furthermore, a single correlation image can be used to assess the characteristic separation distances between features and enable estimates the structure formation frequencies.

Acknowledgments

The authors acknowledge the financial assistance provided to this project by the Australian Research Council through its Linkage Grant scheme and by industrial partner FCT-Combustion.

References

- [1] Abbas, T., Costen, P., Lockwood, F.C. and Romo-Millares, C.A. The effect of particle size on NO formation in a large-scale pulverized coal-fired laboratory furnace: Measurements and Modeling, *Combust. Flame*, **93**, 1993 316-326.
- [2] Adrian, R.J., Particle-imaging techniques for experimental fluid mechanics, *Annu. Rev. Fluid Mech*, **23**, 1991, 261-304.
- [3] Birzer, C.H., Kalt P.A.M. and Nathan G.J. A Methodology for Measuring Particle Clustering from Planar Images, *11th Int. Conf. on Multiphase Flows in Industrial Plants*, 2008
- [4] Birzer, C.H., Kalt P.A.M. and Nathan G.J. The Influence of Jet Precession on Near Field Particle Distributions, in preparation for *The Int. J. of Multiphase Flow*.
- [5] Cassel, H.M., and Leibman, I., The cooperative mechanism in the ignition of dust dispersions, *Combust. Flame* **3**, 1958 467-475.
- [6] Kalt, P.A.M., Birzer, C.H. and Nathan, G.J., Corrections to Facilitate Planar Imaging of Particle Concentration in Particle-Laden Flows using Mie-Scattering Part 1: Collimated Laser Sheets. *Appl. Optics*, **46**(23), 2007, 5823-5834.
- [7] Kalt, P.A.M. and Nathan, G.J., Corrections to Facilitate Planar Imaging of Particle Concentration in Particle-Laden Flows using Mie-Scattering Part 2: Diverging Laser Sheets. *Appl. Optics*, **46**(30) 2007, 7227-7236.
- [8] Keane, R.D., Adrian, R.J. (1992) Theory of cross-correlation analysis of PIV images, *Appl. Scie Res.* **49**, 191-215.
- [9] Smith, N.L., Megalos, N.P., Nathan, G.J., Zhang, D.K., and Smart, J.P., Precessing jet burners for stable and low NOx pulverised fuel flames – preliminary results from small-scale trials *Fuel*. **77**, 1998, pp. 1013-1016
- [10] Zhang, D.K. and Wall, T.F. An analysis of the ignition of coal dust clouds, *Combust. Flame* **92**, 1993, 475-480.
- [11] Zimmer, L., Ikeda, Y., Fujimoto, K. and Nakajima, T., Planar Droplet Sizing for the Characterization of Clusters in an Industrial Gun-Type Burner, *11th Int. Symp. Application of Laser Tech. to Fluid Mech.* 2002
- [12] Zimmer, L., Ikeda, Y., Domann, R. and Hardalupas, Y., Simultaneous LIF and Mie Scattering Measurements for Branch-Like Spray Cluster in Industrial Oil Burner, *40th AIAA Aerospace Sciences Meeting and Exhibit*. 2002